Evolution of the light sensitive defects in high performance multicrystalline silicon wafers

Rune Søndenå[1a] & Marie Syre Wiig[1]

[1]Institute for Energy Technology, Instituttveien 18, 2007 Kjeller, Norway

Sequential degradation measurements have been performed on passivated high performance multicrystalline silicon wafers, first at room temperature under low intensity illumination, followed by a higher intensity illumination at an elevated temperature. The presence of two main degradation mechanisms, affecting the lifetime under different conditions has been demonstrated, namely the well-studied light induced degradation caused by boron-oxygen-complexes, and the less understood light and elevated temperature induced degradation. Light and elevated temperature induced degradation is the main lifetime limiting recombination path when fully activated, but the contribution from boron-oxygen complexes is not negligible. This separation of the two degradation mechanisms might therefore be necessary for proper evaluation of the dominant recombination mechanism. Experiments also show regeneration of the minority carrier lifetimes caused by deactivation of both the lifetime limiting defects at comparable timescales, and under similar illumination and temperature conditions. Wafers from different heights in a high performance multicrystalline silicon ingot has been evaluated to better understand the underlying causes for the different degradation mechanisms. Effects of the iron-boron-splitting on the carrier lifetime are only visible in ungettered wafers.

I. INTRODUCTION

Several defects and impurity complexes in crystalline silicon are sensitive to illumination or charge injection. Firstly, light induced degradation in silicon containing both boron and oxygen (BO-LID) results in a considerable reduction in the minority charge carrier lifetime (lifetime for short) upon illumination due to the activation of BO-complexes as recombination sites[1,2]. Much of the initial lifetime can be recovered and a metastable state with a regenerated high lifetime can be obtained using illumination at elevated temperatures[3]. Secondly, the dissociation of FeB-pairs into Fe_i and B_s species with illumination will also affect the measured lifetime due to the different injection dependencies of the recombination of FeB and Fe_i[4]. Thirdly, an additional degradation mechanism, named light and elevated temperature induced degradation (LeTID), was observed in 2012[5]. This last defect degrades the performance of passivated emitter and rear contacted (PERC) cells considerably, with an efficiency reduction of about 6-12 %$_{relative}$ on cell level[5–9]. Degradation as a function of the height in the brick has previously been reported, indicating slightly less degradation towards the top of the ingots[10,11].

LeTID has been widely studied in the recent years, but the underlying cause is still not identified[7,12,13]. It was first discovered in multicrystalline silicon (mc-Si), but has later also been observed in Czochralski (Cz) and float-zone (FZ) monocrystalline silicon material[12,14]. The initial high lifetime is reduced during prolonged illumination at elevated temperatures, followed by a subsequent regeneration towards the high initial lifetime with continued heating and charge injection[9,13,15]. For modules at field conditions this decay and recovery cycle may take many years, in which they operate at a reduced performance[16,17]. LeTID defects are activated during the contact firing step of a solar cell, when a hydrogen rich dielectric layer is present[18]. Previous studies have found that peak temperatures above approximately 700 °C are

[a]Electronic mail: rune.sondena@ife.no

required to activate LeTID, that the extent of the degradation increases with increasing peak temperatures, and that the extent can also be manipulated by varying the cooling rate[19–22]. Hence, strategies for reducing or removing the effect of LeTID by optimizing the cell process parameters have been found[11,23]. Jensen et al. have demonstrated that it is the hydrogen injection that activate the LeTID, not the high temperature firing process[24]. Despite the relation between hydrogen and the LeTID defect mechanism avoiding or reducing the introduction of hydrogen is not an ideal solution to reduce LeTID in high performance multicrystalline silicon (HPMC-Si) wafers and cells, since hydrogen also has an important beneficial effect of passivating the grain boundary recombination of charge carriers[25,26]. Therefore, further understanding of the defect and its behavior is important to improve the quality of HPMC-Si.

The boron-oxygen complex causing BO-LID was early ruled out as a potential cause for LeTID, despite the similarities in the parameters for lifetime regeneration. The nature of the defect causing LeTID is largely unknown. The involvement of many possible metallic impurities has been evaluated based on solubility and diffusivity of the elements in silicon, and a few potential candidates stand out; particularly Cu, Co, and Ni[27,28]. The involvement of hydrogen, either by itself or in complexes, is suspected due to its importance during the activation of LeTID in the contact firing process[24,27]. In addition an alternative defect model based on boron-hydrogen pairs (B-H) has recently been proposed[29].

Evaluation of the LeTID degradation is made more complicated by the simultaneous presence of BO-LID as well as extended crystal defects, such as grain boundaries, in p-type HPMC-Si wafers. The effective lifetime in silicon wafers is given as the inverse sum of the individual lifetime contributions, as shown in Equation 1,

$$\frac{1}{\tau_{effective}} = \frac{1}{\tau_{LeTID}} + \frac{1}{\tau_{BO}} + \frac{1}{\tau_{crystal\,defects}} + \frac{1}{\tau_{other}} + \frac{1}{\tau_{surface}} \tag{1}$$

where the main contributions to the effective lifetime are τ_{LeTID}, τ_{BO}, and $\tau_{crystal\,defects}$. Contributions from τ_{other} and $\tau_{surface}$ are not influenced by illumination and the contributions are considered minor compared to the former three due to efficient gettering and surface passivation. Luka et al. have reported that the impact of the BO-related degradation on the V_{OC} is minimal in current cells based on HPMC Si wafers[30,31]. Most of the previous work therefore evaluate the total degradation of the carrier lifetime in wafers[9,13,16,32,33] or the performance of cells[6,8,15] using only one illumination step at an elevated temperature. LeTID is then considered the dominant recombination mechanism and other lifetime limiting effects are neglected. However, all the bulk contributions to the lifetime are more visible when evaluating the minority carrier lifetime in surface passivated wafers as the $\tau_{surface}$-term in Equation 1 is minimized. Thus, BO-LID may potentially be more consequential in more advanced cell concepts with higher V_{OC}-values. Significant contributions from the τ_{BO}-, and the $\tau_{crystal\,defects}$-terms in Equation 1 are also expected, especially prior to full activation of the LeTID defect. Thorough analysis of the magnitude of the LeTID as well as its formation kinetics is therefore difficult without first subtracting the contribution of BO-LID from the total degradation. The effect of BO-LID has indeed been accounted for by an initial light soaking at room temperature prior to the LeTID measurements in a few recent papers[30,31,34–36]. In the present work the total degradation in wafers has been measured sequentially, with the aim of separating the effects of the different degradation mechanisms found in HPMC silicon. In addition, the influence of ingot height on the degradation has been evaluated and discussed.

2

II. EXPERIMENTAL DETAILS

Commercially available HPMC-Si wafers from several different heights in an ingot were used in this minority carrier lifetime study on degradation. The wafers are p-type (boron-doped) with a resistivity of approximately 1 Ω-cm. Neighboring wafers from each height in a center brick were processed according to Figure 1a[26]. As-sawn wafers were damage etched in a HNA-solution (HF, nitric acid, acetic acid). Half the wafers were then subjected to a two-sided phosphorus emitter in-diffusion from a gas phase POCl$_3$ source in a tube furnace. Diffusion of metallic impurities towards the emitter region, where they are less harmful to the material quality, during the in-diffusion process is called a gettering process[37]. A hydrogen rich SiN$_X$ anti-reflective coating (ARC) was deposited on both sides before the wafers were subjected to a simulated contact firing process in a belt furnace. The simulated firing process was performed without screen printing of the metal pastes and corresponding contact formation. The high temperature profiles, i.e. the POCl$_3$ emitter in-diffusion and the contact firing profile, are shown in Figure 1b and 1c, respectively. The ARC's and the phosphorus emitter layers were then removed in a new HNA-solution before all the wafers were cleaned and surface passivated using a a-Si:H/SiN$_X$:H-stack deposited by plasma-enhanced chemical vapor deposition. Surface recombination velocities of less than 5 cm/s are routinely obtained using this process[38]. The samples are heated to 230 °C for a total of 20 minutes during the surface passivation process. Injection dependent minority carrier lifetimes were measured on 5 × 5 cm^2 pieces of the wafers using the quasi steady-state photoconductance (QssPC) technique (Sinton lifetime tester WCT-120TS). The lifetime values were measured at 25 °C, and extracted at $\Delta n \approx 0.1 \times p_0$, corresponding to an injection level of about 1.5×10^{15} cm^{-3}.
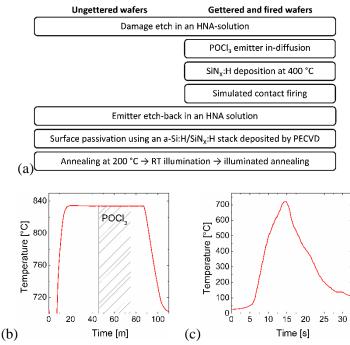

FIG. 1. Two processing routes for each pair of neighboring wafers taken from three different heights in the ingot are shown in a). All wafers are etched together to ensure comparable surface properties. The gettered and fired wafers are exposed to temperature profiles for the phosphorus in-diffusion and the simulated contact firing as shown in b) and c), respectively. The temperature profiles are measured using a thermocouple placed on a wafer during the firing process, and by using thermocouples inside the tube during the emitter in-diffusion.

The sequential degradation study was performed by measuring the lifetime at various time intervals while first illuminating the samples at room temperature (RT) followed by an illuminated annealing sequence. A LED lamp with an intensity of approximately 5 mW/cm^2 for approximately 72 hours was used to induce degradation at RT. The subsequent illuminated annealing was performed by exposing the samples to LED light with an intensity of about 70 mW/cm^2 while heated to 150 °C on a hotplate. The first measurement sequence has been automated[39,40] while the samples were moved manually from the hotplate to the QssPC to measure the lifetime at RT in the second sequence. Phosphor-based white LED light with two peaks between 450 and 800 nm was used in both measurement sequences. Prior to the measurements all wafers were annealed in the dark at 200 °C for 20 minutes to deactivate the BO-defects and obtain a high initial lifetime.[33] The potential effect of this dark annealing step at 200 °C as well as the temperature processing in the PECVD at 230 °C on the LeTID defects has been assumed to be negligible due to the short time[14].

III. RESULTS AND DISCUSSION

The sequential degradation curves in the gettered and fired samples during illumination first at room temperature, and then at an elevated temperature of 150 °C, are shown in Figure 2. High initial lifetimes, τ_0, were ensured by measuring on areas of the wafers with a minimum of dislocation clusters and grain boundaries. Initial lifetimes of just above 700 µs were measured in the wafers from 39 %, 62 %, and 90 % of the ingot height, while a slightly lower τ_0 of about 500 µs was measured for the lower position at 18 % of the height. This reduced lifetime in the lower parts of the ingot may be caused by a reduced grain size in the wafer and therefore an increased grain boundary recombination despite choosing a high lifetime area for the measurements. Photoluminescence images of the approximate areas of the wafers placed over the QssPC-coil are shown in Figure 3 together with injection dependent lifetime curves for four different states along the degradation and recovery curves; The initial lifetime after the annealing process, the BO-degraded lifetime after 72 hours of illumination at room temperature, the lowest lifetime with activated LeTID defects, and the recovered lifetime after illuminated annealing for 8 hours. Illumination at RT causes a degradation over the first 48 to 72 hours, a timescale comparable to that of the BO-degradation seen in p-type Cz-Si[2]. These first degraded lifetimes, τ_{BO}, in the HPMC-Si wafers are about 60-75% of the high initial lifetime, depending on height in the brick. In p-type Cz-Si wafers the degradation caused by BO-defects is considerably stronger. BO-LID in Cz-Si wafers typically exhibits a lifetime decay in two stages with different timescales. Fast and slow recombination centers are responsible for the decay in the first few minutes and the following 48 to 72 hours, respectively[2]. The fast decay was not observed in the HPMC-Si wafers studied here, but the slow decay was observed with a similar time frame as BO-LID in Cz-Si wafers. A similar result was also found in previous study on conventional mc-Si wafers, where the authors only measured a minimal contribution from the fast decay[40]. The initial lifetime in the current HPMC-Si wafers can largely be recovered by a dark anneal at 200 °C. A comparable timescale of the decay in HPMC-Si and Cz-Si under illumination lead us to attribute this initial light induced degradation at room temperature to BO-defects, despite the lack of a clear fast decay the first few minutes of illumination. This assumption is supported by the fact that this first degradation occurring under illumination at room temperature was also observed in ungettered wafers (Fig. 4), where LeTID defects have not been activated by a firing process.

It is worth noting that the lifetimes in the gettered and fired wafers after 72 hours of illumination at room temperature (Fig. 2) were not completely stabilized. Wafers from high positions in the ingots seem to have less stable lifetimes after 72 hours of BO-LID than wafers from lower positions. In addition, a small lowering of the initial lifetime with repeated annealing at 200 °C has been observed. This may be related to LeTID defects through the dark annealing effect[6,14], or to a potential emerging formation of LeTID defects at RT. Vargas et al. have recently reported a very slow degradation following an initial improvement of the carrier lifetime under illumination at RT [41].
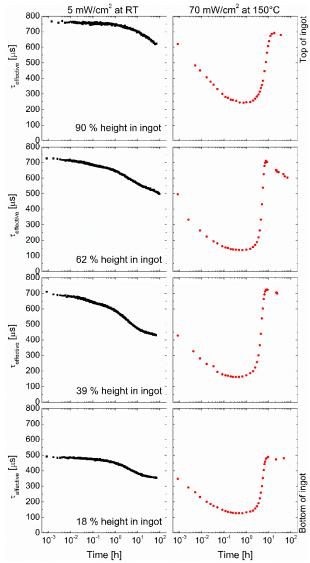

FIG. 2. Sequential lifetime degradation curves in gettered and fired wafers from different heights in the ingot. The BO-LID and the LeTID contributions to the total degradation are shown on the left- and on the right-hand side, respectively.

With increased light intensity and elevated temperatures, a second degradation mechanism is activated in the gettered and fired wafers. Figure 2 shows that within 5-15 minutes of illumination at 150 °C the lifetimes are typically reduced to their minimum values where LeTID defects have been fully activated. In our wafers minimum lifetimes of 130 to 160 μs have been measured. Figure 4 confirms that this second degradation at an elevated temperature was not observed in wafers that have not gone through the firing process. This second degradation is therefore attributed LeTID-defects.
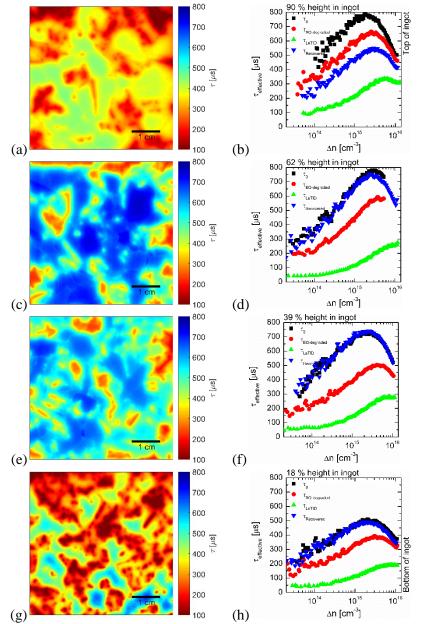
FIG. 3. QssPC calibrated photoluminescence images of the samples from different heights are shown on the left-hand side. Injection dependent lifetime curves for four states along their degradation and recovery curves are shown on the right-hand side; the initial state, the BO-degraded state, the LeTID degraded state, and the recovered state.

After about 1 hour of illuminated annealing a gradual increase in the lifetime started for both the ungettered (Fig. 4), as well as for the gettered and fired wafers (Fig. 2). Much of the initial lifetime can be recovered. As the recovered lifetimes were well above the lifetimes after the first BO-degradation at RT we must conclude that the recovery is a combined effect of deactivating both BO-defects and LeTID-defects. Thus, contributions from two different recombination mechanisms that are deactivated under comparable conditions must be considered when evaluating the kinetics of the regeneration process. Sperber et al. have demonstrated a general decrease in the surface passivation quality of hydrogen rich dielectric layers upon extended illumination and heating potentially explaining the small instability of the

recovered lifetime and the second degradation observed after approximately 20 hours of heating and illumination[42,43].
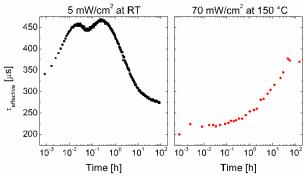

FIG. 4. Sequential lifetime degradation in an ungettered wafer from about 39 % of the ingot height. The BO-degradation is shown on the left-hand side, while on the right-hand side there is no sign of the LeTID when the temperature is increased. Effects of FeB-pair splitting can be seen in the first few minutes of illumination in both measurement sequences.

The degradation and recovery profile in an ungettered wafer, in Figure 4, shows the BO-degradation under illumination at RT, with no additional LeTID degradation at elevated temperatures. This confirms that a high temperature step is required to activate LeTID defects. In addition, the ungettered wafer showed an increase in in the lifetime in the first few minutes of illumination after the initial dark anneal at 200 °C. This effect can be explained by the presence of a reasonable amount of interstitial iron, which is not present in the gettered wafers. Splitting of FeB-pairs may give rise to such an increase of the minority carrier lifetime at an injection level of 1.5×10^{15} cm^{-3}. Minimal effects of iron-boron-pair splitting are expected in the gettered and fired wafers as interstitial iron is quite effectively removed from the intragrain areas during phosphorus gettering[44].
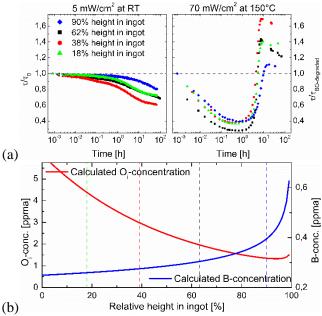

FIG. 5. Normalized lifetime curves in gettered and fired wafers for both BO-LID and LeTID are shown in a). Oxygen levels and boron concentrations in b) are calculated according the Scheil equation and the model proposed by Tang et al., respectively[45,46]. Approximate positions of the wafers studied in this work are indicated with dashed lines.

7

Separating the degradation caused by the two main defect mechanisms relevant for gettered and fired wafers allow for an improved evaluation of the lifetime evolution. Figure 5a shows the normalized degradation and recovery curves for the gettered and fired samples. The first decay caused by BO-LID is normalized towards the initial lifetime, τ_0, while the second decay is normalized towards the BO-stabilized lifetime, τ_{BO}, i.e. approximately equal to the first measurement in the LeTID sequence. The lowest lifetime measured for each sample is as low as $0.2 - 0.3 \times \tau_0$, agreeing with some of the previous lifetime studies of LeTID degradation[13,19]. However, the magnitude of the LeTID will depend on the firing temperature[21,22]. When comparing the three wafers with comparable initial lifetimes, i.e. the wafers from 39 %, 62 %, and 90 % relative heights in the ingot, we see that the BO-related degradation typically decreases with increasing height in the ingot. This corresponds well with the expected reduction of oxygen content towards the top of a HPMC-Si ingot[45,47]. The wafer from the lower position, however, demonstrates less BO-related degradation than expected. Only after 6 minutes of illumination the BO-defect becomes the dominating recombination path. An increased amount of grain boundaries in this wafer from the lower position reduces the initial lifetime somewhat compared to the samples from higher in the brick, causing an underestimation of the amount of BO-LID recombination centers present. Crystal defects may in fact be an important lifetime limiting recombination mechanism prior to illumination when the contributions from the BO-LID and the LeTID terms in Equation 1 are small. Variations in the crystal structure may therefore affect the amount of degradation attributed to the different light induced degradation mechanisms. A presence of structural defects limiting the lifetime in all the wafers studied may also explain why we do not observe the fast decay caused by BO-LID in HPMC-Si.

The normalized LeTID curves obtained under illuminated annealing show no clear correlation with the height in the brick. We can, however, conclude that there is no correlation between LeTID and the expected interstitial oxygen concentration. As mentioned above, continued degradation after 72 hours of illumination at room temperature shows lifetime curves that are not completely stabilized. Increased instability towards the top of the brick can be seen in Figure 2. If this instability is caused by LeTID forming already at room temperature it could indicate increasing LeTID with increasing height in the ingot. Increasing LeTID towards the top of ingots indicates that the responsible defect is related to a defect or impurity element that increases in concentration towards the top of the ingot, e.g. metallic impurities, dopants, or crystal defects. Several possible defect mechanisms for LeTID are therefore still relevant. Certain metallic impurities or crystal defects, may be responsible for the LeTID[12,23,27,28]. As LeTID is activated in a firing process with a hydrogen rich ARC present, hydrogen is believed to play a major role. A recent defect model for LeTID, proposing boron and hydrogen pairs[29], may also explain the trend of increasing LeTID towards the top of high performance multicrystalline silicon ingots as observed in this work.

The current study illustrates the challenges arising from degradation studies on HPMC-Si wafers; In addition to challenges in separating the effects of BO-LID and LeTID, the extended defects, i.e. grain boundaries and dislocation clusters, may severely affect the effective lifetime and, therefore, also the degree of degradation attributed the different light sensitive recombination mechanisms found in a wafer.

IV. SUMMARY

Three different light sensitive degradation mechanisms have been demonstrated in surface passivated HPMC-Si wafers subjected to two different processing routes. Interstitial iron is efficiently removed in the gettering process during phosphorus emitter in-diffusion. The effect of iron-boron pair splitting on the

minority carrier lifetime was therefore only visible in ungettered wafers. Boron-oxygen related light induced degradation was, however, visible in both ungettered wafers as well as in wafers that have gone through a gettering process and a simulated firing process with a hydrogen rich ARC present. A second, more severe degradation, occurring under illumination at elevated temperatures was seen only in this last group of wafers where LeTID defects had been activated in a firing process.

The degradation contributions caused by BO-defects and the less understood LeTID-defects are in this work separated using a sequential measurement routine. First the sample is degraded with respect to the BO-defects by illumination at room temperature, followed by illumination at higher temperatures to activate the LeTID defects. The degradation curves in the wafers with comparable initial lifetimes indicate that the BO-related degradation decreases with increasing height in the ingot, in agreement with an expected decrease in the levels of interstitial oxygen. No clear trend can be seen for LeTID. After about one hour of illumination using 70 mW/cm^2 at a temperature of 150 °C the minority carrier lifetimes started to recover. This regeneration process is assumed to be a combined effect where the both BO- and LeTID-defects are deactivated with respect to their recombination activity.

Acknowledgements

[1] K. Bothe and J. Schmidt, Appl. Phys. Lett. **87**, 262108 (2005).

[2] T.U. Nærland, H. Haug, H. Angelskår, R. Søndenå, E.S. Marstein, and L. Arnberg, IEEE J. Photovoltaics **3**, 1265 (2013).

[3] A. Herguth and G. Hahn, J. Appl. Phys. **108**, 114509 (2010).

[4] D. Macdonald, J. Tan, and T. Trupke, J. Appl. Phys. **103**, 73710 (2008).

[5] K. Ramspeck, S. Zimmermann, H. Nagel, A. Metz, Y. Gassenbauer, B. Birkmann, and A. Seidel, in *27th EUPVSEC* (Frankfurt, Germany, 2012).

[6] C. Chan, T.H. Fung, M. Abbott, D. Payne, A. Wenham, B. Hallam, R. Chen, and S. Wenham, Sol. Rapid Res. Lett. **1**, 1600028 (2017).

[7] P.P. Altermatt, Z. Xiong, Q. He, W. Deng, F. Ye, Y. Yang, Y. Chen, Z. Feng, P.J. Verlinden, A. Liu, D.H. Macdonald, T. Luka, D. Lausch, M. Turek, C. Hagendorf, H. Wagner-Mohnsen, J. Schön, W. Kwapil, F. Frühauf, O. Breitenstein, E.E. Looney, T. Buonassisi, D.B. Needleman, C.M. Jackson, A.R. Arehart, S.A. Ringel, K.R. McIntosh, M.D. Abbott, B.A. Sudbury, A. Zuschlag, C. Winter, D. Skorka, G. Hahn, D. Chung, B. Mitchell, P. Geelan-Small, and T. Trupke, Sol. Energy in press (2018).

[8] D.N.R. Payne, C.E. Chan, B.J. Hallam, B. Hoex, M.D. Abbott, S.R. Wenham, and D.M. Bagnall, Sol. Energy Mater. Sol. Cells **158**, 102 (2016).

[9] A. Zuschlag, D. Skorka, and G. Hahn, Prog. Photovoltaics **25**, 545 (2017).

[10] K. Petter, K. Hübener, F. Kersten, M. Bartzsch, F. Fertig, and J. Müller, in *9th Int. Work. Cryst. Si Sol. Cells* (Tempe, Arizona, USA, 2016).

[11] F. Kersten, P. Engelhart, H.-C. Ploigt, F. Stenzel, K. Petter, A. Szpeth, M. Bartzsch, A. Stekolnikov, M. Scherff, J. Heitmann, and J.W. Müller, in *31st EUPVSEC* (Hamburg, Germany, 2015).

[12] T. Niewelt, F. Schindler, W. Kwapil, R. Eberle, J. Schön, and M.C. Schubert, Prog. Photovoltaics Res. Appl. **26**, 533 (2018).

[13] M.A. Jensen, A. Morishige, J. Hofstetter, and T. Buonassisi, IEEE J. Photovoltaics **7**, 980 (2017).

[14] D. Chen, M. Kim, B. V Stefani, B.J. Hallam, M.D. Abbott, C.E. Chan, R. Chen, D.N.R. Payne, N. Nampalli, A. Ciesla, T.H. Fung, K. Kim, and S.R. Wenham, Sol. Energy Mater. Sol. Cells **172**, 293 (2017).

[15] F. Kersten, P. Engelhart, H.-C. Ploigt, A. Stekolnikov, T. Lindner, F. Stenzel, M. Bartzsch, A. Szpeth, K. Petter, J. Heitmann, and J.W. Müller, Sol. Energy Mater. Sol. Cells **142**, 83 (2015).

[16] J.M. Fritz, A. Zuschlag, D. Skorka, A. Schmid, and G. Hahn, Energy Procedia **124**, 718 (2017).

[17] F. Kersten, F. Fertig, K. Petter, B. Klöter, E. Herzog, M.B. Strobel, J. Heitmann, and J.W. Müller, Energy Procedia **124**, 540 (2017).

[18] C. Vargas, K. Kim, G. Coletti, D. Payne, C. Chan, S. Wenham, and Z. Hameiri, IEEE J. Photovoltaics **8**, 413 (2018).

[19] D. Bredemeier, D. Walter, S. Herlufsen, and J. Schmidt, Energy Procedia **92**, 773 (2016).

[20] R. Eberle, W. Kwapil, F. Schindler, M.C. Schubert, and S.W. Glunz, Phys. Status Solidi-Rapid Res. Lett. **10**, 861 (2016).

[21] C.E. Chan, D.N.R. Payne, B.J. Hallam, M.D. Abbott, T.H. Fung, A.M. Wenham, B.S. Tjahjono, and S.R. Wenham, IEEE J. Photovoltaics **6**, 1473 (2016).

[22] A. Herguth, P. Keller, and N. Mundhaas, AIP Conf. Proc. **1999**, 130007 (2018).

[23] K. Nakayashiki, J. Hofstetter, A.E. Morishige, T.-T.A. Li, D.B. Needleman, and M. Jensen, IEEE J. Photovoltaics **6**, 860 (2016).

[24] M.A. Jensen, A. Zuschlag, S. Wieghold, D. Skorka, A.E. Morishige, G. Hahn, and T. Buonassisi, J. Appl. Phys. **124**, 85701 (2018).

[25] M.S. Wiig, H. Haug, R. Søndenå, and E.S. Marstein, Energy Procedia **124**, 215 (2017).

[26] K. Adamczyk, R. Søndenå, G. Stokkan, E. Looney, M. Jensen, B. Lai, M. Rinio, and M. Di Sabatino, J. Appl. Phys. **123**, 55705 (2018).

[27] D. Bredemeier, D.C. Walter, and J. Schmidt, Sol. Rapid Res. Lett. **2**, 1700159 (2018).

[28] M.A. Jensen, A.E. Morishige, S. Chakraborty, R. Sharma, H.S. Laine, B. Lai, V. Rose, A. Youssef, E.E. Looney, S. Wieghold, J.R. Poindexter, J.-P. Correa-Baena, T. Felisca, H. Savin, J.B. Li, and T. Buonassisi, IEEE J. Photovoltaics **8**, 448 (2018).

[29] T.H. Fung, M. Kim, D. Chen, C.E. Chan, B.J. Hallam, R. Chen, D.N.R. Payne, A. Ciesla, S.R. Wenham, and M.D. Abbott, Sol. Energy Mater. Sol. Cells **184**, 48 (2018).

[30] T. Luka, S. Grosser, C. Hagendorf, K. Ramspeck, and M. Turek, Sol. Energy Mater. Sol. Cells **158**, 43 (2016).

[31] T. Luka, M. Turek, C. Kranert, S. Grosser, and C. Hagendorf, Energy Procedia **124**, 759 (2017).

[32] D. Bredemeier, D. Walter, S. Herlufsen, and J. Schmidt, AIP Adv. **6**, (2016).

[33] H.C. Sio, H. Wang, Q. Wang, C. Sun, W. Chen, H. Jin, and D. Macdonald, Sol. Energy Mater. Sol. Cells **182**, 98 (2018).

[34] M. Kim, D. Chen, M. Abbott, S. Wenham, and B. Hallam, AIP Conf. Proc. **1999**, 130010 (2018).

[35] F. Fertig, K. Krauß, and S. Rein, Phys. Status Solidi – Rapid Res. Lett. **9**, 41 (2014).

[36] K. Krauß, A.A. Brand, F. Fertig, S. Rein, and J. Nekarda, IEEE J. Photovoltaics **6**, 1427 (2016).

[37] M. Syre, S. Karazhanov, B.R. Olaisen, A. Holt, and B.G. Svensson, J. Appl. Phys. **110**, 24912 (2011).

[38] H. Haug, R. Søndenå, M.S. Wiig, and E.S. Marstein, Energy Procedia **124**, 47 (2017).

[39] T.U. Nærland, Characterization of Light Induced Degradation in Crystalline Silicon, 2013.

[40] R. Søndenå and A. Ghaderi, in *EUPVSEC* (Amsterdam, Netherlands, 2014).

[41] C. Vargas, G. Coletti, C. Chan, D. Payne, and Z. Hameiri, Sol. Energy Mater. Sol. Cells **189**, 166 (2019).

[42] D. Sperber, A. Heilemann, A. Herguth, and G. Hahn, IEEE J. Photovoltaics **7**, 463 (2017).

[43] D. Sperber, A. Graf, D. Skorka, A. Herguth, and G. Hahn, IEEE J. Photovoltaics **7**, 1627 (2017).

[44] M.S. Wiig, K. Adamczyk, H. Haug, K.E. Ekstrøm, and R. Søndenå, Energy Procedia **92**, 886 (2016).

[45] K. Tang, M. Syvertsen, R. Fagerberg, C. Modanese, and M. Di Sabatino, in 6th *Int. Work. Cryst. Si Sol. Cells* (Aix-Les-Baines, France, 2012).

[46] R. Søndenå, H. Haug, A. Song, C.-C. Hsueh, and J.O. Odden, AIP Conf. Proc. **1999**, 130016 (2018).

[47] A.-K. Søiland, J.O. Odden, B. Sandberg, K. Friestad, J. Håkedal, E. Enebakk, and S. Braathen, in 6th *Int. Work. Cryst. Si Sol. Cells* (Aix-Les-Bains, France, 2012).